Proceedings of the International MultiConference of Engineers and Computer Scientists 2014 Vol II,
IMECS 2014, March 12 - 14, 2014, Hong Kong

State-Space Battery Modeling for Smart Battery Management System

T. O. Ting, Ka Lok Man, Nan Zhang, Chi-Un Lei, Chao Lu

***Abstract*—Battery Management System (BMS) requires an indefinite accurate model. With an aging model, the lifetime of a battery can be precisely predicted. The mathematical model in terms of state variables is presented in this preliminary work involving smart BMS system. This work is crucial as the state space model is able to mimic the complex dynamic behavior of a battery system. A numerical case study is done to verify the model obtained through mathematical derivations by adopting the prominent RC battery model from literature. More works have to be carried out to investigate the application of the model in terms of predicting the state of charge (SoC) of a battery system in order to prolong its lifetime, and thereby saving us substantial cost.**

***Index Terms*—Battery aging, Battery Management System (BMS), battery modeling, state-of-charge, state space.**

I. Introduction

THE understanding of a battery system is essential before efficient management system could be designed [1], [2]. Hence, a generic tool to describe the battery performance under a wide variety of conditions and applications is highly desirable [3]. As such, the electrical modeling is able to provide such a tool that enables visualization of the processes occurring inside rechargeable batteries. Only with the presence of these generic models could new battery management algorithms be developed for reliable performance. These algorithms control the operation and maintain the performance of battery packs. The ultimate aim is to prolong battery life and ensuring reliable safety. Battery modeling is done in many ways depending on the types of battery.

Ultimately, with the battery models aim to determine state of charge (SoC). However, the complexity of the nonlinear electrochemical processes has been a great barrier to modeling this dynamic process accurately. The accurate determination of SoC will enable utilization of the battery for optimal performance, long lifetime, and prevent irreversible physical damage to the battery. Solution to SoC via neural networks [4] and fuzzy logic [5] have been difficult and costly for online implementation due to large computation, causing the battery pack controller to be heavily loaded. However, this can be a good alternative in the near future due to the increased computational power of processing chips alongside their declining cost.

Manuscript received December 10, 2013; revised January 23, 2014. This work was supported by Xi'an Jiaotong-Liverpool University under RDF-13-01-13.

T. O. Ting is with the Department of Electrical and Electronic Engineering, Xian Jiaotong-Liverpool University, China. Email: toting@xjtlu.edu.cn

K. L. Man and N. Zhang are with the Department of Computer Science and Software Engineering, Xian Jiaotong-Liverpool University, China. Email: ka.man, nan.zhang@xjtlu.edu.cn

C.-U. Lei is with the Department of Electrical and Electronic Engineering, The University of Hong Kong, Hong Kong. Email: culei@eee.hku.hk

C. Lu is with Purdue University, West Lafayette, IN. Email: eeluchao@gmail.com

Model-based state-estimation has been proposed in [6], [7]. In [7] a state-estimation model has been utilized for the determination of optimized charging current using Genetic Algorithm (GA). In [8] ant colony algorithm is applied to determine the charging current in each stage to reduce charging time. In control theories, the well-known Kalman filter [9] have been applied successfully for both state observation and prediction problems [6]. In this work, a mathematical derivation leading to a state space model is presented. The basic schematic model is in fact adopted from [6], [7]. Although the conclusion is the same, we presented more analysis in the form of state variables. The rest of the paper is organized as follows. Section II discusses the factors of battery aging. Section III outlines the aging characteristics from measurement data. A mathematical model is derived in Section IV, which is followed by state space model in Section V, and finally the conclusions are derived in Section VI.

II. Battery Aging

Identification of key aging parameters in battery models can validate degradation hypotheses and provide a foundation for estimation of battery status, e.g. State of Health (SOH). In brief, aging and degradation of batteries can be caused by capacity fading (the loss of battery charging/discharging capacity over time) as well as power fading (the loss of absorbing and delivering electrical power). From another perspective, power fading and energy fading are associated with impedance rise and capacity loss, respectively. Detailed discussion of typical aging effects can be found in [10]. A few major effects are outlined in the following subsections.

A. Thermal Degradation

The performance of a battery is significantly affected by temperature. For e.g., Lithium battery can effectively operate between $-30°C$ and $52°C$. When the temperature drops below $-30°C$, diffusion and chemical reactions become inactive and thus battery impedance increased dramatically. On the other hand, when the temperature rises above $60°C$, the battery has a significant capacity loss. And eventually if the temperature rises above $85°C$, the battery could be damaged easily. Chemical reactions in batteries grow exponentially when the temperature increases. Meanwhile, since vigorous chemical reactions generate excessive heat, the battery could also broke down if the if heat from batteries is not properly managed.

B. Physical Damage

Battery aging can also be caused by electrode fracture and fatigue. In existing literatures, a specific electrode model and a diffusion-induced stress model have been proposed for investigation [11]. Results showed that the output voltage does not change significantly, however it increasingly accumulates stress.

C. Particles Accumulation

Solid Electrolyte Interphase (SEI) are formed on the surface of electrodes when the battery charges, and in particular, when electrode starts to react with the electrolyte. SEI absorbs mobilized Lithium ions and slows down the transportation of ions between electrode and electrolyte. These formed crystalline introduce power fading and capacity fading. In the case of low and high current densities, moss and dendrite are formed on the surface of negative electrode. These substances reduces surface area of electrodes for reactions, and thus causing battery fading.

III. Aging Characterization and Regulation through Measured Data

Measurements are needed in order to accurately characterize aging in batteries. To investigate the cycle life capabilities of lithium ion battery cells during fast charging, cycle life tests have been carried out at different constant charge current rates. Through measurement results, cycle life models have been developed to predict the battery cycle ability. The analysis indicates that the cycle life of the battery degrades when the charge current rate increases. In addition, the measurement of battery impedance via electrochemical impedance spectroscopy (EIS) and the current-pulse technique [12] helps in determining battery health.

In order to ensure a uniform temperature during battery operations, maintaining battery performance, and eventually prolong the battery lifetime, real-time temperature sensing and monitoring systems as well as cooling systems are needed [13], [14], [15]. In addition, in order to improve cycle stability and battery capacity, thick anodes (e.g. about 1 mm) are adopted for Li-ion batteries. These anodes consist of vertically aligned carbon nanotubes which are coated with silicon and carbon [16].

A. Aging Models

Aging parameters in Lithium-ion batteries vary with different current rates, working temperatures and depths of discharge. For example, in order to model the thermal characteristics of the battery that causes battery aging, it is necessary to model the generation of heat inside the battery, heat transfer between battery and the environment, and the reactivity of chemical reactions with respect to the temperature [17]. In particular, in order to correctly model the thermal distribution and characteristics of battery packs, lumped thermal models are formulated to model the ohmic heating in battery cell packs [18]. The aging parameters can be applied for early aging detection. Through early detection and appropriate maintenance, performance of battery cells can be significantly improved. Detection can be done by analyzing real-time data from operations of batteries (e.g. voltage and current data from lithium-ion cells). In [12], battery aging detection is done based on the sequential clustering of battery packs. During operations, a derived fuzzy model is used to predict operation performance and detect the aged battery via similarity comparisons, with respect to the ideal situation.

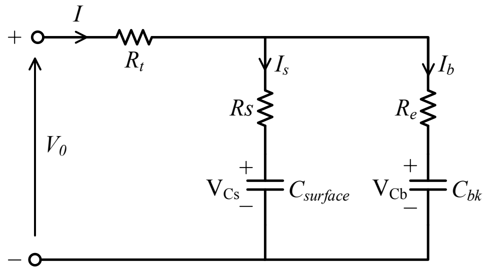

Fig. 1. Schematic of RC battery model

IV. Battery Model

Several battery models existed over the past years. Each of these models varies in term of its complexity and applications. In this work, a dynamical battery model is adopted, consisting of state variable equations, from [6]. The schematic representation of this model is shown in Fig. 1. In this model, there exists a bulk capacitor C_{bk} that acts as a energy storage component in the form of charge, a capacitor that models the surface capacitance and diffusion effects within the cell $C_{surface}$, a terminal surface R_t, surface resistance R_s, and end resistance R_e. The voltages across both capacitors are denoted as V_{Cb} and V_{Cs}, respectively.

A. Mathematical Derivations of Battery Model

In this derivation, we aim to form a state-space model consisting of the state variables V_{Cb}, V_{Cs} and V_0. State variables are mathematical description of the "state" of a dynamic system. In practice, the state of a system is used to determine its future behaviour. Models that consist of paired first-order differential equations are in state-variable form.

Following the voltages and currents illustrated in Fig. 1, the terminal voltage V_0 can be expressed as:

$$V_0 = IR_t + I_b R_e + V_{Cb}, \tag{1}$$

which is similar to

$$V_0 = IR_t + I_b R_s + V_{Cs}. \tag{2}$$

By equating the (1) and (2), and after simple algebraic manipulation results in

$$I_b R_e = I_s R_s + V_{Cs} - V_{Cb}. \tag{3}$$

From Kirchoff's laws, $I = I_b + I_s$,

$$I_s = I - I_b, \tag{4}$$

Substituting (4) into (3) yields

$$I_b(R_e + R_s) = IR_s + V_{Cs} - V_{Cb}. \tag{5}$$

By assuming a slow varying C_{bk}, that is $I_b = C_{bk}\dot{V}_{Cb}$ (from basic formula of $i = C\frac{\partial V}{\partial t}$) and substituting into (5), the following equation is obtained after rearrangement

$$\dot{V}_{Cb} = \frac{IR_s}{C_{bk}(R_e + R_s)} + \frac{V_{Cs}}{C_{bk}(R_e + R_s)}$$

ISBN: 978-988-19253-3-6
ISSN: 2078-0958 (Print); ISSN: 2078-0966 (Online)

$$-\frac{V_{Cb}}{C_{bk}(R_e+R_s)}, \tag{6}$$

By applying a similar derivation, the rate of change of the surface capacitor voltage, derived also from (1) and (2) as

$$\dot{V}_{Cs} = \frac{IR_e}{C_{surface}(R_e+R_s)} - \frac{V_{Cs}}{C_{surface}(R_e+R_s)} + \frac{V_{Cb}}{C_{surface}(R_e+R_s)}. \tag{7}$$

By assuming $A = \frac{1}{C_{bk}(R_e+R_s)}$ and $B = \frac{1}{C_{surface}(R_e+R_s)}$, (6) and (7) can be written as

$$\dot{V}_{Cb} = A \cdot IR_s + A \cdot V_{Cs} - A \cdot V_{Cb} \tag{8}$$

and

$$\dot{V}_{Cs} = B \cdot IR_e - B \cdot V_{Cs} + B \cdot V_{Cb}, \tag{9}$$

respectively. Further, (8) and (9) can be combined to form a state variable relating voltages V_{Cs} and V_{Cb} and current flow I, which is

$$\begin{bmatrix} \dot{V}_{Cb} \\ \dot{V}_{Cs} \end{bmatrix} = \begin{bmatrix} -A & A \\ B & -B \end{bmatrix} \begin{bmatrix} V_{Cb} \\ V_{Cs} \end{bmatrix} + \begin{bmatrix} A \cdot R_s \\ B \cdot R_e \end{bmatrix} I. \tag{10}$$

Next, the output voltage is derived from (1) and (2). By adding both equations,

$$2V_0 = 2IR_t + I_b R_e + I_s R_s + V_{Cb} + V_{Cs}. \tag{11}$$

By substituting $I_b = \frac{R_s}{R_s+R_e}$ and $I_s = \frac{R_e}{R_s+R_e}$ into (11), it is further simplified as

$$V_0 = \frac{V_{Cb}+V_{Cs}}{2} + \left(R_t + \frac{R_e R_s}{R_e+R_s}\right) I \tag{12}$$

By taking the time derivative of the output voltage and assuming $dI/dt \approx 0$ (this simply mean that the change rate of terminal current can be ignored when implemented digitally). Hence we get

$$\dot{V}_0 = \frac{\dot{V}_{Cb}+\dot{V}_{Cs}}{2}. \tag{13}$$

By substituting the values obtained earlier in (8) and (9) into (13) results in

$$2\dot{V}_0 = (-A+B)V_{Cb} + (A-B)V_{Cs} + (AR_s+BR_e)I. \tag{14}$$

Then, by solving for V_{Cs} from (12) we obtain

$$V_{Cs} = 2V_0 - 2(R_t + \frac{R_e R_s}{R_e+R_s})I - V_{Cb}, \tag{15}$$

and after substitution into (14) yields

$$\dot{V}_0 = (-A+B)V_{Cb} + (A-B)V_0 + \left[A\left(0.5R_s+R_t+D\right) + B\left(0.5R_e-R_t-D\right)\right] I. \tag{16}$$

Finally, the complete state variable network is obtained by integrating (16) into (10), thus the complete state variable description of the network is obtained as

$$\begin{bmatrix} \dot{V}_{Cb} \\ \dot{V}_{Cs} \\ \dot{V}_0 \end{bmatrix} = \begin{bmatrix} -A & A & 0 \\ B & -B & 0 \\ (-A+B) & 0 & (A-B) \end{bmatrix} \cdot \begin{bmatrix} V_{Cb} \\ V_{Cs} \\ V_0 \end{bmatrix} + \begin{bmatrix} A \cdot R_s \\ B \cdot R_e \\ A\left(0.5R_s - R_t - D\right) + B\left(0.5R_e + R_t + D\right) \end{bmatrix} I. \tag{17}$$

whereby constants A, B and D have been given earlier and hereby restated as

$$\begin{bmatrix} A \\ B \\ D \end{bmatrix} = \begin{bmatrix} \frac{1}{C_{bk}(R_e+R_s)} \\ \frac{1}{C_{surface}(R_e+R_s)} \\ \frac{R_e R_s}{R_e+R_s} \end{bmatrix}.$$

This completes the initial derivation of a battery model.

V. State Space Modeling

Considering the effect of both time and charging current leading to the time and current dependent model for C_{bk} makes the state equations to be nonlinear. Further, we adopt the formula for C_{bk} from [7], given as

$$C_{bk} = \begin{cases} C_0 & t \le t_0 \\ -K_1 I(t-t_0) - K_2(t-t_0) + C_0 & t \ge t_0 \end{cases} \tag{18}$$

whereby K_1 and K_2 are given in [7] and not included here as we deem this as not important in this work. This C_{bk} can be augmented (or included) into the existing state variable of (10). As mentioned, the value of C_{bk} shows the ability of the battery to store charge. As such, C_{bk} is a good factor for consideration in determining the State of Health (SoH) of the battery. Assuming the rate of change of C_{bk} over a sampling interval is negligible; in other words $\dot{C}_{bk} = \partial C_{bk}/\partial t = 0$. Therefore, the battery model, specified by (19) can be re-written as

$$\begin{bmatrix} \dot{V}_{Cb} \\ \dot{V}_{Cs} \\ \dot{V}_0 \\ \dot{C}_{bk} \end{bmatrix} = \begin{bmatrix} -A & A & 0 & 0 \\ B & -B & 0 & 0 \\ (-A+B) & 0 & (A-B) & 0 \\ 0 & 0 & 0 & 0 \end{bmatrix} \begin{bmatrix} V_{Cb} \\ V_{Cs} \\ V_0 \\ C_{bk} \end{bmatrix} + \begin{bmatrix} A \cdot R_s \\ B \cdot R_e \\ A\left(0.5R_s - R_t - D\right) + B\left(0.5R_e + R_t + D\right) \\ 0 \end{bmatrix} I, \tag{19}$$

with the output $y(t)$ given as

$$y(t) = \begin{bmatrix} V_{Cb} \\ V_{Cs} \\ V_0 \\ C_{bk} \end{bmatrix}. \tag{20}$$

Based on control theories, a lumped linear network can be written in the form

$$\dot{x}(t) = \mathbf{A}x(t) + \mathbf{B}u(t),$$
$$y(t) = \mathbf{C}x(t) + \mathbf{D}u(t).$$

By comparison of the above pair state variables, and substituting all resistor and capacitor values (see Table I) the values $\mathbf{A}$, $\mathbf{B}$, $\mathbf{C}$ and $\mathbf{D}$ are calculated as follows

$$\mathbf{A} = \begin{bmatrix} -0.001508 & 0.001508 & 0 & 0 \\ 1.6238379 & -1.6238379 & 0 & 0 \\ 1.6223291 & 0 & -1.6223291 & 0 \\ 0 & 0 & 0 & 0 \end{bmatrix},$$

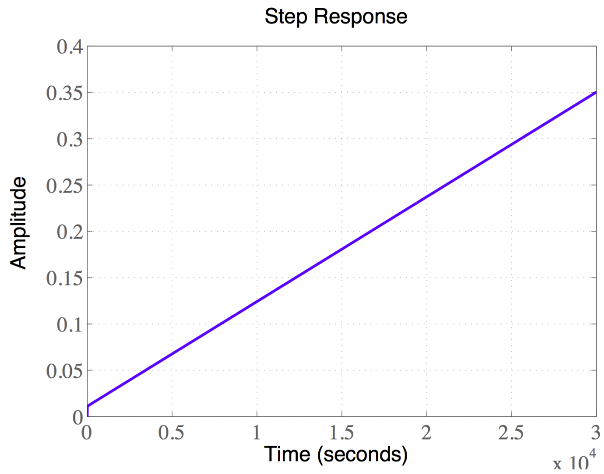

Fig. 2. Unit step response for Battery Model

$$\mathbf{B} = \begin{bmatrix} 0.000005657847553 \\ 0.006089392278651 \\ 0.010542685882214 \\ 0 \end{bmatrix},$$

$$\mathbf{C} = \begin{bmatrix} 0 & 0 & 1 & 0 \end{bmatrix},$$

$$\mathbf{D} = \begin{bmatrix} 0 \end{bmatrix}.$$

Further, the above state space variables are transformed to a transfer function, $G(s)$. This is done by using `ss2tf` function in Matlab, and thereby yielding

$$G(s) = \frac{0.01054s^3 + 0.0171s^2 + 2.981 \times 10^{-5}s}{s^4 + 3.248s^3 + 2.637s^2 - 1.144 \times 10^{-18}s} \quad (21)$$

The plot of the unit step response for the gain in (21) is given in Fig. 2. Basically, it shows that the open circuit terminal voltage V_0 in Fig. 1 increases linearly during charging operation. This behaviour is consistent with the linear cell discharge characteristics illustrated in Fig. 15 of [6]. This somehow validates the results obtained from the mathematical analysis done. However, we deem it necessary to further explore the model in the aim of tackling SoC. This will be one priority task for future work.

TABLE I
PARAMETERS FOR CELL MODEL [6]

C_{bk}	$C_{surface}$	R_e	R_s	R_t
88372.83 F	82.11 F	0.00375Ω	0.00375Ω	0.002745Ω

VI. CONCLUSION

In this work, the factors of battery aging are discussed in detail. Subsequently, we successfully obtain the state variables of the RC model that represents a battery in terms of Mathematical derivations. The derivations come to a conclusion that there exists four state variables relevant to battery model. Further, based on control theories, we successfully plotted the response of the system, depicting a linearly increasing characteristic. With this state-estimation model, the technique such as Kalman filter can be applied in the aim of estimating state of charge. We leave this as an open option for future investigation.

ACKNOWLEDGMENT

The authors would like to acknowledge the support from Xi'an Jiaotong-Liverpool University under RDF-13-01-13

REFERENCES

[1] C. Chen, K. L. Man, T. O. Ting, C. U. Lei, T. Krilavicius, T. T. Jeong, J. K. Seon, S. U. Guan, and P. W. H. Wong, "Design and realization of a smart battery management system," in *Proc of Intl MultiConference of Engineers and Computer Scientists*, vol. 2, 2012, pp. 1173–1176.

[2] K. L. Man, K. Wan, T. O. Ting, C. Chen, T. Krilavičius, J. Chang, and S. H. Poon, "Towards a hybrid approach to soc estimation for a smart battery management system (bms) and battery supported cyber-physical systems (cps)," in *2nd Baltic Congress on Future Internet Communications (BCFIC)*, 2012, pp. 113–116.

[3] P. H. L. Notten and D. Danilov, "From battery modeling to battery management," in *2011 IEEE 33rd International Telecommunications Energy Conference (INTELEC)*, 2011, pp. 1–8.

[4] C. C. Chan, E. W. C. Lo, and S. Weixiang, "Available capacity computation model based on artificial neural network for lead-acid batteries in electric vehicles," *J. Power Sources*, vol. 87, no. 1, pp. 201–204, 2000.

[5] P. Singh, C. F. Jr, and D. Reisner, "Fuzzy logic modelling of state-of-charge and available capacity of nickel/metal hydride batteries," *J. Power Sources*, vol. 136, no. 2, pp. 322–333, 2004.

[6] B. S. Bhangu, P. Bentley, D. A. Stone, and C. M. Bingham, "Nonlinear observers for predicting state-of-charge and state-of-health of lead-acid batteries for hybrid-electric vehicles," *IEEE Trans. Veh. Technol.*, vol. 54, no. 3, pp. 783–794, 2005.

[7] H. Saberi and F. R. Salmasi, "Genetic optimization of charging current for lead-acid batteries in hybrid electric vehicles," in *International Conference on Electrical Machines and Systems, ICEMS*, 2007, pp. 2028–2032.

[8] Y.-H. Liu, J.-H. Teng, and Y.-C. Lin, "Search for an optimal rapid charging pattern for lithium-ion batteries using ant colony system algorithm," *IEEE Trans. Ind. Electron.*, vol. 52, no. 5, pp. 1328–1336, 2005.

[9] R. E. Kalman *et al.*, "A new approach to linear filtering and prediction problems," *Journal of Basic Engineering*, vol. 82, no. 1, pp. 35–45, 1960.

[10] J. Vetter, P. Novák, M. R. Wagner, C. Veit, K. C. Möller, J. O. Besenhard, M. Winter, M. Wohlfahrt-Mehrens, C. Vogler, and A. Hammouche, "Ageing mechanisms in lithium-ion batteries," *J. Power Sources*, vol. 147, no. 1–2, pp. 269–281, 2005.

[11] J. Christensen, "Modeling diffusion-induced stress in li-ion cells with porous electrodes," *J. Electrochem. Soc.*, vol. 157, no. 3, pp. A366–A380, 2010.

[12] W. Waag, S. Käbitz, and D. U. Sauer, "Experimental investigation of the lithium-ion battery impedance characteristic at various conditions and aging states and its influence on the application," *Appl. Energy*, vol. 102, pp. 885–897, 2013.

[13] R. Kizilel, R. Sabbah, J. R. Selman, and S. Al-Hallaj, "An alternative cooling system to enhance the safety of li-ion battery packs," *J. Power Sources*, vol. 194, no. 2, pp. 1105–1112, 2009.

[14] R. Mahamud and C. Park, "Reciprocating air flow for li-ion battery thermal management to improve temperature uniformity," *J. Power Sources*, vol. 196, no. 13, pp. 5685–5696, 2011.

[15] S. Al-Hallaj and J. R. Selman, "Thermal modeling of secondary lithium batteries for electric vehicle/hybrid electric vehicle applications," *J. Power Sources*, vol. 110, no. 2, pp. 341–348, 2002.

[16] K. Evanoff, J. Khan, A. A. Balandin, A. Magasinski, W. J. Ready, T. F. Fuller, and G. Yushin, "Towards ultrathick battery electrodes: Aligned carbon nanotube-enabled architecture," *Adv. Mater.*, vol. 24, no. 4, pp. 533–537, 2012.

[17] M. Doyle, T. Fuller, and J. Newman, "Modeling of galvanostatic charge and discharge of the lithium/ polymer/insertion cell," *J. Electrochem. Soc.*, vol. 140, no. 6, pp. 1526–1533, 1993.

[18] K. Smith and C.-Y. Wang, "Power and thermal characterization of a lithium-ion battery pack for hybrid-electric vehicles," *J. Power Sources*, vol. 160, no. 1, pp. 662–673, 2006.